ELSEVIER

Journal of Molecular Catalysis A: Chemical 158 (2000) 189–197

JOURNAL OF MOLECULAR CATALYSIS A: CHEMICAL

www.elsevier.com/locate/molcata

Olefin epoxidation by mono and bisperoxo complexes of Mo(VI): a density functional model study

Ilya V. Yudanov [1], Cristiana Di Valentin [2], Philip Gisdakis, Notker Rösch *

Institut für Physikalische und Theoretische Chemie, Technische Universität München, D-85747 Garching, Germany

Abstract

Olefin epoxidation by Mo(VI) peroxo complexes was computationally investigated (DFT B3LYP) for various monoperoxo models $X_2MoO(O_2)(H_2O)(NH_3)$ with anionic ligands X and for the experimentally known complex $MoO(O_2)(dipic)(H_2O)$. All these monoperoxo complexes exhibit higher barriers for direct oxygen transfer to ethylene than the reference bisperoxo complex $MoO(O_2)_2(H_2O)(NH_3)$ with the same base ligand configuration; the most electronegative ligands X induce the lowest barriers. A molecular orbital analysis reveals factors that govern the activity of the peroxo ligand and corroborates the electrophilic character of the attack of a peroxo group on the olefin.

Keywords: Density functional calculations; Epoxidation; Peroxo complexes; Molybdenum; Transition states

1. Introduction

Peroxo complexes of early transition metals in their highest oxidation states like Ti(IV), V(V), Mo(VI), W(VI), and Re(VII) attract much interest due to their activity in oxygen transfer reactions, in particular olefin epoxidation [1–3]. Quantum chemical calculations using a density functional (DF) approach are a valuable tool [4] for investigating olefin epoxidation by transition metal peroxo complexes as they provide important information on the reaction mechanism, including the reaction energetics, structure of reactive intermediates and transition states, and activation barriers for conceivable competitive pathways of oxygen transfer [5–8]. In particular, the DF computations combined with experimental studies [6,7] can shed light on the epoxidation by the catalytic system methyltrioxorhenium/H_2O_2 [9] where a bisperoxo complex $CH_3ReO(O_2)_2(H_2O)$ [10] is considered as key intermediate.

* Corresponding author. Tel.: +49-89-289-13620; fax: +49-89-289-13622.

E-mail address: roesch@ch.tum.de (N. Rösch).

[1] Permanent address: Boreskov Institute of Catalysis, Siberian Branch of Russian Academy of Sciences, 630090 Novosibirsk, Russia.

[2] Permanent address: Dipartimento di Chimica Organica, Università degli Studi di Pavia, V. le Taramelli 10, I-27100 Pavia, Italy.

1381-1169/00/$ - see front matter
PII: S1381-1169(00)00065-0

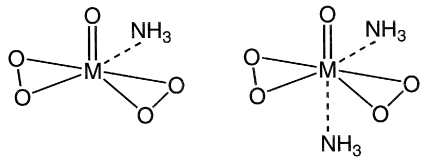

1a **1b**

Recently, a comparative DF study [11] was carried out on the epoxidation activity of a series of bisperoxo complexes of Cr, Mo, and W (**1a**,**1b**) using ethylene as a model olefin substrate. Various complexes $MO(O_2)_2L_1L_2$ (M = Cr, Mo, W) with different combinations of base ligands L_1 and L_2 have been experimentally characterized (for a review, see Ref. [12]). The Mo and W complexes have been found to stoichiometrically epoxidize alkenes. The complex $MoO(O_2)_2$(hmpt) (hmpt = hexamethylphosphoric triamide) [13] attracted much attention although there are indications that its tungsten analogue $WO(O_2)_2$(hmpt) is a more effective epoxidant [14]. The epoxidation ability of all these complexes is inhibited by strongly coordinating solvents [13,14]. This finding has led to a long-term discussion of the reaction mechanism. Mimoun initially proposed [1,13] that the olefin substrate first binds to the metal center and then inserts into a metal–peroxo bond forming a metallacycle intermediate. In this model, the inhibiting effect was interpreted to result from a solvent molecule occupying a free coordination position at the metal center. Later investigations favored a mechanism that involves the direct attack of the substrate on a peroxo oxygen center [14–16]. In that case, the effect of the solvent ligand was attributed to reduced electrophilicity of the peroxo group due to induction of electron density from this ligand to the peroxo group via the metal center. According to our calculations [11], a direct oxygen transfer from a peroxo complex to olefin exhibits a significantly lower activation barrier than insertion. We showed also that the activation barriers increase dramatically when an additional base ligand coordinates (cf. **1a** and **1b**). Complexes of Cr, Mo, W exhibit similar effects of additional base ligands, but the calculated activation barriers for complexes of analogous structure decrease along the series Cr > Mo > W. This finding is in line with the known poor epoxidation activity of Cr complexes and the higher activity of W species compared to Mo [14].

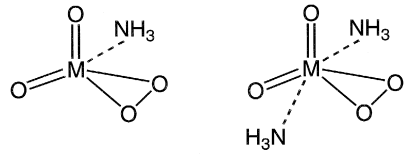

2a **2b**

Much less is known about epoxidation by monoperoxo complexes of Mo or W although a number of complexes have been characterized [12] and new synthesis of such species for stereoselective epoxidation is a matter of considerable interest [17]. In our previous study [11], the activity of Cr/Mo/W bisperoxo complexes **1a** and **1b** was compared to that of monoperoxo complexes, **2a** and **2b**, formed by abstraction of an oxygen center from one of the peroxo groups of a bisperoxo complex. Monoperoxo species were calculated to exhibit higher activation barriers for ethylene epoxidation than the corresponding bisperoxo complexes; e.g. **2a** has a barrier of 19 kcal/mol compared to 14 kcal/mol of **1a** (M = Mo). However, it remained open how other types of anionic ligands, e.g. chlorine or alkyloxide, affect the reactivity of the metal peroxo group.

Here we computationally characterize a series of monoperoxo model complexes $X_2MoO(O_2)(H_2O)(NH_3)$ with various anionic ligands X. First, we consider the calculated geometry and electronic structure of these complexes; then we compare their activity in the epoxidation of olefins via calculations of the corresponding

transition states and activation barriers for ethylene as model olefin. As reference for comparison, we will employ the bisperoxo complex $MoO(O_2)_2(H_2O)(NH_3)$ that has the same configuration of base ligands H_2O and NH_3. We will leave aside steric and environment effects and focus on electronic effects of ligands on the properties of the moieties $Mo(O_2)$.

2. Computational details

In the calculations [18], we employed the hybrid B3LYP DF method [19,20]. The core shells of Mo (except 4s and 4p) were replaced by the LANL2 effective core potential [21]. The corresponding basis set [21], which describes the outermost core (4s and 4p) and the valence shells of Mo, was used in the contraction (441/2111/31). For the main group elements we employed a 6–31G* basis set [22]. Geometry optimizations of intermediates and transition states were performed without any symmetry constraints. The transition state structures were searched by numerically estimating the matrix of second-order energy derivatives at every optimization step and by requiring exactly one eigenvalue of this matrix to be negative. The barrier heights were evaluated in single-point fashion with the Mo basis set augmented by two polarization f-exponents (0.79063 and 0.27345 [11]) and the basis set for main group elements extended to 6–311G(d,p) [23].

In the preceding studies of Re and Mo oxo and peroxo complexes [6,24], the zero-point energy corrections were shown to uniformly shift the calculated reaction energies and reaction barriers by small positive values. However, in no case did they change the qualitative picture when reactivities of different intermediates were compared. Therefore, in the present study, we refrained from applying zero-point energy corrections to reaction energies and barrier heights.

3. Results and discussion

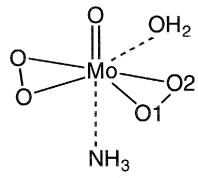

3

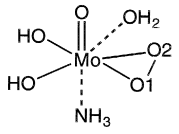

4a

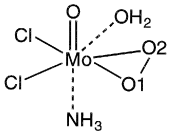

4b

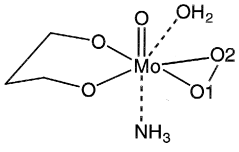

4c

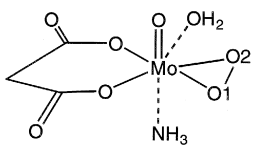

4d

3.1. Model complexes

The bisperoxo complex **3** will be used as a reference for the evaluation of the activity of monoperoxo species; it differs from similar systems (**1b**) studied previously [11] by substitution of the equatorial ammonia ligand by water. The model monoperoxo complexes **4a–4d** are derived from **3** by replacing one of the peroxo groups by two monodentate or one bidentate anionic ligands. In complexes **4a** and **4b**, one of the peroxo groups is replaced by a pair of hydroxide and chlorine ligands, respectively. The bidentate organic ligands of structures **4c** and **4d** are used to model alkyloxide or carboxylate functions, respectively, at the metal center. All model complexes exhibit a pentagonal–bipyramidal structure that is typical for the known oxomono and oxobisperoxo complexes of Mo

[12]. The binding energies of the axial base ligand NH_3 to the Mo center are given in Table 1. Previous computational studies on the activity of peroxo complexes of Re [6,7], Ti [8] and the Cr/Mo/W triad [11] have shown that the peroxo species with lower coordination numbers exhibit lower activation barriers for the oxygen transfer than corresponding coordinatively saturated base adducts. Nevertheless, due to a thermodynamic stabilization, the latter yield the lowest lying transition states by the absolute energy. Therefore, in the present study, we consider only seven-coordinated Mo peroxo species as coordinatively saturated and thermodynamically most stable.

The selected optimized geometry parameters of the model structures are given in Table 1. The calculated structure of the bisperoxo complex **3** is in reasonable agreement with the available X-ray crystal structures for $MoO(O_2)_2(H_2O)_2$ [25], $MoO(O_2)_2(hmpt)(H_2O)$ and $MoO(O_2)_2(hmpt)(py)$ [26] (py = pyridine); in the latter two complexes hmpt is an equatorial ligand. The calculated O–O distance, 1.446 Å, of the peroxo group is very close to the experimental values of $MoO(O_2)_2(H_2O)_2$ and $MoO(O_2)_2(hmpt)(Py)$, 1.45 and 1.44 Å, respectively, but slightly shorter than in $MoO(O_2)_2(hmpt)(H_2O)$, 1.50 Å. Computations yield slightly longer distances between the Mo center and atoms of the peroxo group; cf. the calculated values 1.94 and 1.97 Å for Mo–O1 and Mo–O2, respectively, with experimental results of 1.90 and 1.92 Å for $MoO(O_2)_2(H_2O)_2$ and $MoO(O_2)_2(hmpt)(Py)$. Also the calculated $Mo–O_{oxo}$ distance is by 0.05–0.06 Å longer than those derived from X-ray data. The largest deviation of calculated and experimental results is for the

Table 1
Calculated characteristics of the Mo bisperoxo complex **3** and the monoperoxo complexes **4a–4d**
Distances r in Å; binding energies $\Delta E(NH_3)$ of NH_3 ligand to the complex and activation barriers $\Delta E^{\#}$ for ethylene epoxidation in kcal/mol; NBO atomic charges q in e; energy of $\sigma^*(O–O)$ level in eV.

	3	**4a**	**4b**	**4c**	**4d**
Geometry of complex					
r(O–O)	1.446	1.430	1.413	1.429	1.425
r(Mo–O1)	1.94	1.97	1.97	1.97	1.95
r(Mo–O2)	1.97	1.95	1.95	1.95	1.96
r(Mo=O)	1.71	1.70	1.69	1.71	1.70
$r(Mo–OH_2)$	2.32	2.31	2.29	2.36	2.29
r(Mo–N)	2.44	2.47	2.48	2.43	2.45
$\Delta E(NH_3)$	−17.4	−14.0	−18.7	−15.3	−19.1
NBO atomic charges					
q(O1)	−0.37	−0.35	−0.31	−0.35	−0.32
q(O2)	−0.42	−0.39	−0.35	−0.37	−0.36
q(O–O)	−0.79	−0.74	−0.66	−0.72	−0.68
$q(NH_3)$	0.15	0.14	0.14	0.15	0.15
$q(H_2O)$	0.15	0.13	0.16	0.13	0.16
$\sigma^*(O–O)$[a]	1.6	2.0	1.3	2.2	1.1
Geometry of transition state					
r(O–O)	1.84	1.79	1.75	1.79	1.79
r(Mo–O1)	2.01	2.08	2.08	2.10	2.04
r(Mo–O2)	1.86	1.83	1.82	1.82	1.82
r(O–C1)	2.06	2.07	2.14	2.07	2.09
r(O–C2)	2.10	2.03	2.07	1.99	2.09
r(C–C)[b]	1.36	1.36	1.36	1.37	1.36
Activation barrier $\Delta E^{\#}$	18.5	23.1	22.6	25.1	20.2

[a] $\sigma^*(O–O)$ is not the LUMO of the complex; it lies slightly above the manifold of vacant Mo d-levels.
[b] r(C–C) for gas phase C_2H_4 is calculated to 1.33 Å.

distance Mo–O_{water} of the equatorial ligands H_2O and hmpt (calc. 2.32 Å; exp. 2.08 [25] and 2.04–2.06 [26], respectively). This discrepancy can be rationalized by intermolecular interactions in the crystal structure, e.g. with a co-crystallized ether molecule in the case of $MoO(O_2)_2(H_2O)_2$ [25]. A similar deviation between a computed and experimental value of a metal–O_{water} distance (by about 0.2 Å) was previously found for the complex $CH_3ReO(O_2)_2(H_2O)$ [6]; there, the calculations based on a more realistic model that included an ether molecule yielded a shortened metal–O_{water} distance in significantly better agreement with the experiment. The distance from Mo to the axial N center, 2.44 Å, almost coincides with the experimental Mo–N distance in $MoO(O_2)_2$(hmpt)(Py).

If a peroxo group is replaced by other anionic ligands X, only rather small structural changes are calculated for the rest of the complex, at most by 0.04 Å for the distances between the Mo center and base ligands (Table 1). Note a shortening of the O—O bond distance in the peroxo group of the monoperoxo complexes compared to the bisperoxo species **3**. Although these changes are small, they indicate a strengthening of the O—O bond, concomitant with the higher calculated epoxidation activation barriers (see discussion below).

3.2. Epoxidation transition states

To study the epoxidation activity of the various intermediates described above, we calculated in each case the transition states of the oxygen transfer to the model olefin, i.e. ethylene. We focus on the direct oxygen transfer mechanism where the olefin double bond is attached directly by an oxygen center of the peroxo group. The activation barriers are calculated with respect to the corresponding ''free'' complexes and an ethylene molecule. In the following, we will not discuss the insertion mechanism [1,13] (see Section 1) since the previous studies of Re [6] and Cr/Mo/W [11] peroxo complexes at the same level of computation showed this [2 + 2] insertion to exhibit significantly higher activation barriers than a direct transfer.

The calculated transition states for the complexes under study have a number of features in common and, in general, resemble the structures of transition states of direct oxygen transfer for other d^0 transition metal peroxo complexes of Re, Ti and Cr/Mo/W [6–8,11]. It was shown that the lowest lying transition structures exhibit a spiro orientation of the ethylene unit, i.e. the CCO plane is almost orthogonal to the MOO plane formed by the metal peroxo group. In Table 1, we present the calculated activation barriers for the attack by ethylene molecule of the less negative ''front'' oxygen, i.e. that center of the peroxo group which is distant from the equatorial base ligand. Attack of the other, ''back'' oxygen center exhibits always a somewhat higher activation barrier [6–8,11].

The structure of the ethylene moiety in the calculated transition states is only slightly distorted from the gas phase structure: the C—C bond in the transition state is elongated by about 0.03 Å. All transition states represent a synchronous approach of ethylene to the peroxo moiety with almost equal distances between the carbon atoms and the attacked oxygen center, ranging from 2.0 to 2.1 Å. Similar synchronous transition states were calculated at the same level of computation for the epoxidation of ethylene by other transition metal peroxo complexes (Re, Ti, Cr/Mo/W [6–8,11]) as well as for the epoxidation of 1-pentene [27] and allyl alcohol [28] by peroxyformic acid. The distance between the Mo center and the attacked oxygen, Mo–O1, increases in the transition state by 0.07–0.13 Å whereas the distance Mo–O2 decreases by 0.11–0.13 Å (Table 1). The most dramatic changes on the way to the transition state occur in the structure of the peroxo moiety: the O—O distance lengthens from 1.41–1.45 Å in the ''free'' complexes to 1.75–1.84 Å in the transition states (Table 1).

All calculated monoperoxo species exhibit higher activation barriers than the bisperoxo complex **3**. The lowest activation barrier for a monoperoxo species, 20.2 kcal/mol, is calculated for **4d**, the highest barrier, 25.1 kcal/mol, for **4c**. Note that the corresponding anionic ligands X of these two complexes differ very little; ligand X is connected to Mo by two alkyloxide functions in **4c** and by two carboxylate functions in **4d**. The complexes with hydroxide ligands, **4a**, and chlorine ligands, **4b**, exhibit the activation barriers of 23.1 and 22.6 kcal/mol, respectively.

3.3. Orbital and population analysis

Olefin epoxidation by a d^0 metal peroxo complexes is generally considered as an electrophilic attack of the oxygen on the olefin [1,2]. This view is based on the fact that the peroxo and alkylperoxo complexes react faster with the electron-rich olefins, e.g. with highly alkyl substituted species. The computational results also yield a lower activation energy for epoxidation of the electron-rich alkenes; for instance, the calculated activation barriers for the oxygen transfer from the complex $H_3CReO(O_2)_2$ to ethylene and tetramethylethylene are 12.4 and 6.3 kcal/mol, respectively [7]. In a recent experimental study with peroxo compounds of V, Mo, and W, the electrophilic nature of peroxo oxygen centers was also probed by sulfoxidation of thianthrene 5-oxide, in which an oxygen center of a peroxo complex attacks the electron-rich sulfide group rather than the electron-poor sulfoxide group [29]. In the present calculations, the electrophilic character of the oxygen transfer is manifested through the electron density transfer in the transition state, about 0.2 e, from ethylene to the peroxo complex. In terms of the molecular orbital structure, this is reflected by the interaction of the bonding π(C–C) HOMO of ethylene and the unoccupied anti-bonding σ^*(O–O) orbital of the peroxo complex that leads to the breaking of the O–O bond in peroxo group [7,11]. Thus, the energy of the unoccupied anti-bonding σ^*(O–O) level is one of the factors that determine the activity of the peroxo complex in oxygen transfer [7], since it reflects the ability of the peroxo group to accept additional electron density from the olefin π orbital.

The energies of molecular orbitals with the σ^*(O–O) dominating contribution are given in Table 1. Among the monoperoxo complexes **4a–4d**, there is an obvious correlation between the energy of the σ^*(O–O) orbital and the calculated activation barrier: **4d** exhibits the lowest position of σ^*(O–O) and the lowest activation barrier, while the highest σ^*(O–O) energy of **4c** corresponds to the highest barrier. The charges of the peroxo group given by a natural bond orbital (NBO) analysis [30] also correlate with the height of activation barrier (Table 1): the more electrophilic peroxo groups of **4b** and **4d** yield the lowest barriers.

The bisperoxo complex **3** constitutes a special case in the above analysis. The peroxo groups of the monoperoxo complexes are more electrophilic than those of **3**, if judged by the NBO charges (for all monoperoxo species). Also, the energies of the σ^*(O–O) orbital of **4b** and **4d** lie lower than that of **3**. Nevertheless, **3** exhibits the lowest activation barrier of ethylene epoxidation, 18.5 kcal/mol (Table 1). Concomitantly, as already mentioned, the O–O distance of the peroxo groups of **3** is the longest among the systems under study, 1.446 Å (Table 1).

To rationalize the changes in O–O bond, it is useful to consider the orbital structure of the peroxo ligand in more detail; see Fig. 1 where the orbitals are classified according to the dominant σ and π contribution of the peroxo group as well as its bonding or anti-bonding character with respect to the O–O bond. Evidently, the distribution of electron density between the metal center and the peroxo ligand determines the strength of O–O bond in the peroxo group as well as the strength of M–O bonds between metal center and peroxo group. The higher the

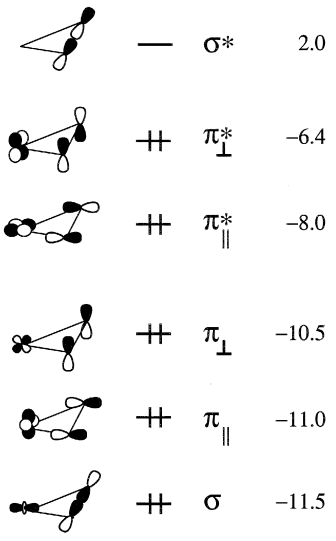

Fig. 1. Orbital structure of a peroxo group coordinated to a d^0 transition metal center. The orbital energies (in eV) are given as calculated for model complex **4a**.

metal contribution to the occupied levels $\pi^*_\perp$ and $\pi^*_\parallel$, the smaller is the anti-bonding O—O character of these orbitals and the stronger the O—O bond. Metal contributions to the orbitals σ, $\pi_\parallel$ and $\pi_\perp$, with O—O bonding character have the opposite effect. According to the population analysis (Table 1), the anionic ligands of complexes **4a–4d** withdraw electron density from the peroxo group via the Mo center. The concomitant decrease of O—O bond length is consistent with the conclusion that the anti-bonding levels of peroxo group are more affected by this process and the decrease of O—O anti-bonding contribution leads to a shorter O—O bond. The highest orbitals with dominant contributions of the anionic ligands in the monoperoxo species are close in energy to the O—O anti-bonding levels $\pi^*_\perp$ and $\pi^*_\parallel$ and strongly mix with them. Thus, there are two competitive effects of anionic ligands in the monoperoxo complexes. First, more electronegative ligands like chlorine or carboxylate render the peroxo group more electrophilic and thus increasing their epoxidation activity. Second, a reduced O—O anti-bonding population leads to a slightly stronger O—O bond and to a higher reaction barrier. The balance of these two effects, which obviously have different weight factors, determines the activity of the peroxo group in the epoxidation process. It seems as if the first effect is more important than the second one. Comparing the calculated barriers of the monoperoxo species, one notes that the more electrophilic species **4b** and **4d** exhibit the lowest barriers while they also feature the shortest O—O distances. Of course, the variations of O—O distances within the monoperoxo family **4a–4d** are really small. However, the second effect can be invoked to rationalize the lower activation barrier of the bisperoxo complex **3**.

Among the closely related complexes considered in the present work the interaction between the Mo center and the peroxo ligand seems to have a more or less constant effect on the reaction activity. At least no clear trends can be observed, neither in the M—O bond lengths nor in the results of the NBO analysis of these bonds. However, variations of the metal–peroxo interaction become important when, for example, the oxidation activity of a ''side-on'' $M(O_2)$ peroxo group is compared to that of an ''end-on'' MOOR hydroperoxo (or alkylperoxo) species [8].

3.4. *$MoO(O_2)(dipic)(H_2O)$ complex*

Finally, we consider the monoperoxo complex $MoO(O_2)(dipic)(H_2O)$ (dipic = dipicolinate) (**5**), which has been experimentally characterized [31]; however, no epoxidation activity was reported for it [12].

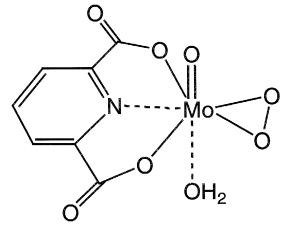

5

This complex with its tridentate picolinate ligand is structurally different from the model complexes **4a–4d**, in particular, by the coordination of the bases at the metal center. The calculated geometry parameters of complex **5** are in good agreement with the X-ray data [31]; especially the parameters of the Mo peroxo group agree quite well: O–O 1.438 (exp. 1.447) Å, Mo–O 1.95 (1.91) Å. The distances from the metal to the base centers, Mo–N and Mo–O_{water}, are 2.17 (2.12) and 2.49 (2.29) Å, respectively. The distance Mo–O_{water} is probably calculated too short since the model does not include a hydrogen bond that is formed between the water ligand and a carboxylate group of a neighboring complex in the crystal structure [31]. The binding energy of the axial water ligand to the Mo center is −19.5 kcal/mol and thus comparable if not larger than the binding energy of the axial base ligand NH_3 in the complexes **4a–4d** (Table 1). The calculated activation barrier for ethylene epoxidation is 21.7 kcal/mol; this value is quite close to the result for model system **4d**, which also contains a ligand with two carboxylate functions. Just as for the other monoperoxo species considered this activation barrier is higher than that for the bisperoxo reference complex **3**.

4. Conclusions

Epoxidation of olefins by Mo(VI) peroxo complexes was investigated using a hybrid DFT method (B3LYP). The epoxidation activity of various monoperoxo complexes $X_2MoO(O_2)(H_2O)(NH_3)$ with different anionic ligands X was compared to the activity of the bisperoxo reference complex $MoO(O_2)_2(H_2O)(NH_3)$ that has the same configuration of base ligands as the monoperoxo model complexes. All monoperoxo species studied feature higher barriers than the bisperoxo reference complex. This finding indicates that bisperoxo Mo species would be a better choice for synthesis of new complexes intended as catalysts for the selective epoxidation of olefins. In line with the electrophilic character of the attack of the peroxo group on the olefin double bond, the lowest barriers among the monoperoxo species are calculated for the more electronegative anionic ligands X, like chlorine and carboxylate. In all complexes studied the Mo center is seven-coordinated and even the lowest calculated activation barrier, i.e. that of the bisperoxo complex $MoO(O_2)_2(H_2O)(NH_3)$, 18.5 kcal/mol, is significantly higher than the barriers calculated previously at the same level of theory for various coordinatively saturated Ti hydroperoxo, 13–15 kcal/mol [8], and Re peroxo species, 13–16 [7].

Acknowledgements

We thank P. Hofmann, H. Rothfuss and J.H. Teles for the helpful discussions. This work was supported by the German Bundesministerium für Bildung, Wissenschaft, Forschung und Technologie (grant no. 03D0050B), INTAS-RFBR (IR-97-1071), and the Fonds der Chemischen Industrie.

References

[1] H. Mimoun, in: S. Patai (Ed.), Chemistry of Peroxides, Wiley, Chichester, 1983, p. 463, Chap. 15.
[2] K.A. Jørgensen, Chem. Rev. 89 (1989) 431.
[3] C.C. Romão, F.E. Kühn, W.A. Herrmann, Chem. Rev. 97 (1997) 3197.
[4] A. Görling, S.B. Trickey, P. Gisdakis, N. Rösch, in: J. Brown, P. Hofmann (Eds.), Topics in Organometallic Chemistry 4 Springer, Heidelberg, 1999, p. 109.
[5] Y.D. Wu, D.K.W. Lai, J. Org. Chem. 60 (1995) 673.
[6] P. Gisdakis, S. Antonczak, S. Köstlmeier, W.A. Herrmann, N. Rösch, Angew. Chem. Int. Ed. 37 (1998) 2211.
[7] F.E. Kühn, A.M. Santos, P.W. Roesky, E. Herdtweck, W. Scherer, P. Gisdakis, I.V. Yudanov, C. Di Valentin, N. Rösch, Chem. Eur. J. 5 (1999) 3603.
[8] I.V. Yudanov, P. Gisdakis, C. Di Valentin, N. Rösch, Eur. J. Inorg. Chem., (1999) 2135.
[9] W.A. Herrmann, R.W. Fischer, D.W. Marz, Angew. Chem. Int. Ed. Engl. 30 (1991) 1638.
[10] W.A. Herrmann, R.W. Fischer, W. Scherer, M.U. Rauch, Angew. Chem. Int. Ed. Engl. 32 (1993) 1157.

[11] C. Di Valentin, P. Gisdakis, I.V. Yudanov, N. Rösch, J. Org. Chem. (2000) in press.
[12] M.H. Dickman, M.T. Pope, Chem. Rev. 94 (1994) 569.
[13] H. Mimoun, I.S.d. Roch, L. Sajus, Tetrahedron 26 (1970) 37.
[14] G. Amato, A. Arcoria, F.P. Ballistreri, G.A. Tomasseli, O. Bortolini, V. Conte, F. Di Furia, G. Modena, G. Valle, J. Mol. Catal. 37 (1986) 165.
[15] S. Camprestini, F. Di Furia, G. Modena, O. Bortolini, J. Org. Chem. 53 (1988) 5721.
[16] E.P. Talsi, K.V. Shalyaev, K.I. Zamaraev, J. Mol. Catal. 83 (1993) 347.
[17] H. Rothfuß, P. Hofmann, unpublished results.
[18] M.J. Frisch, G.W. Trucks, H.B. Schlegel, P.M.W. Gill, B.G. Johnson, M.A. Robb, J.R. Cheeseman, T. Keith, G.A. Petersson, J.A. Montgomery, K. Raghavachari, M.A. Al-Laham, V.G. Zakrzewski, J.V. Ortiz, J.B. Foresman, J. Cioslowski, B.B. Stefanov, A. Nanayakkara, M. Challacombe, C.Y. Peng, P.Y. Ayala, W. Chen, M.W. Wong, J.L. Andres, E.S. Replogle, R. Gomperts, R.L. Martin, D.J. Fox, J.S. Binkley, D.J. Defrees, J. Baker, J.P. Stewart, M. Head-Gordon, C. Gonzalez, J.A. Pople, Gaussian 94, Revision D.4, Gaussian, Pittsburgh, PA, 1995.
[19] A.D. Becke, J. Chem. Phys. 98 (1993) 5648.
[20] C. Lee, W. Yang, R.G. Parr, Phys. Rev. B 37 (1988) 785.
[21] P.J. Hay, W.R. Wadt, J. Chem. Phys. 82 (1985) 299.
[22] W.J. Hehre, R. Ditchfield, J.A. Pople, J. Chem. Phys. 56 (1972) 2257.
[23] R. Krishnan, J. Binkley, R. Seeger, J. Pople, J. Chem. Phys. 72 (1980) 650.
[24] P. Gisdakis, S. Antonczak, N. Rösch, Organometallics 18 (1999) 5044.
[25] C.B. Shoemaker, D.P. Shoemaker, L.V. McAfee, C.W. DeKock, Acta Cryst. C 41 (1985) 347.
[26] P.J.-M. Le Carpentier, R. Schlupp, R. Weiss, Acta Cryst. B 28 (1972) 1278.
[27] D.A. Singleton, S.R. Merrigan, J. Liu, K.N. Houk, J. Am. Chem. Soc. 119 (1997) 3385.
[28] R.D. Bach, C.M. Estévez, J.E. Winter, M.N. Glukhovtsev, J. Am. Chem. Soc. 120 (1998) 680.
[29] W. Adam, D. Golsch, J. Sundermeyer, G. Wahl, Chem. Ber. 129 (1996) 1177.
[30] A.E. Reed, L.A. Curtiss, F. Weinhold, Chem. Rev. 88 (1988) 899.
[31] S.E. Jakobson, R. Tang, F. Mares, Inorg. Chem. 17 (1978) 3055.